Novel Rotary Inchworm Motors

Firas N. Sammoura

EECS 245: Introduction to MEMS
Department of Electrical and Computer Science
University of California, Berkeley, CA 94720
Email: firas@newton.berkeley.edu

Abstract

In this paper, we will demonstrate a family of novel Rotary Inchworm motors using four gap-closing actuators (GCA). Design issues, fabrication process, and expected operation of several rotary motors will be described. The motor is to be batch fabricated using Seth Holler's Silicon-on-Insulator (SOI) plus hinges process. An output torque of the order of nN-m with a torque density in the range of nN-m/mm^2 is theoretically expected when the motor is operated at 30V. A typical Inchworm Rotary motor would measure 1mmx1mmx60μm when the rotor diameter is 200μm. An application of this motor to wave Mickey Mouse's hand is suggested.

I. Introduction

The continuous depletion of natural resources has made it mandatory to fabricate devices as tiny as possible [8]. Micro-Electro Mechanical Systems, or MEMS, has thus established itself as a field that uses lithographic and other precision manufacturing techniques to fabricate appliances on the micro-scale. Such micro devices include a variety of miniaturized sensors and actuators that have a wide range of technological applications such as accelerometers, biosensors, optical switches... One kind of these mini-actuators is the micro rotary motor [6]. The design of micro rotary motors has been the topic of many recent publications [3]. The on-going research in this area aims at designing micro motors with high torque, optimal efficiency, and maximum power density. Proposed applications of such rotary motors include their use as micro pumps and compressors for biomedical applications, micro coolers for microprocessors, and actuators for micro robots [7].

Most of the previous designs of micro rotary motors have used electrostatic forces as the means to thrust the motor [6]. Muller et al. have designed and fabricated several IC-processed electrostatic micro motors. The stators and rotors of these motors were fabricated from polysilicon with a thickness of 1.5μm. Rotors of diameter ranging from 60 to 120μm have been tested up to 100V and output torques of the order of pN-m was reported [3]. Sniegowski et al. demonstrated another version of surface micromachined microengine at Sandia National Laboratory where two sets of linear comb-drive actuators have been implemented to drive the output gear. The linear motion of the comb-drive has been converted into rotary motion via linkages pinned into the output gear. This microengine has been fabricated from polysilicon on one wafer using standard surface micromachinig techniques. The microengines were tested up to 100V and angular speeds up to 300,000 rpm were reported [1, 4, 5]. Pister et al. have demonstrated a linear inchworm motor with a theoretical force of 1mN/mm^2 at 30V [2].

In this paper, four inchworm motors using gap-closing actuators (GCA) are going to be used to drive a free moving rotor. The rotor and the GCA's are to be batch fabricated in Silicon-on-Insulator (SOI) wafers plus hinges with an aspect ratio of approximately 25:1. This will provide higher power density and high torque rotary motors. One layer of polysilicon is to be deposited on top and patterned to constrain the rotor from pulling out of its axle. It will be shown that such rotary inchworm motors are capable of generating torques of the order of nN-m at 30V. A torque density in the range of nN-m/mm^2 is expected. Finally application of this motor to wave a Mickey Mouse's hand is suggested where the motor and the Mickey Mouse are fabricated using SOI plus hinges process.

II. Design

II.1 Description of the Fabrication Process Selected:

The Electrostatic Rotary Inchworm motor is to be fabricated using Deep Reactive Ion Etching (DRIE) of a Silicon Wafer. This process is capable of achieving high aspect ratio structures up to 25:1 (sidewall angles 90 ± 2°). DRIE consists of alternating processes of plasma etching and deposition of protective polymer layers on the sidewalls (Teflon for instance). A layer of silicon dioxide (SiO_2) is used as a limiting layer for etching since silicon to silicon dioxide selectivity ranges from 120 to 200:1 [6]. After the motor, the

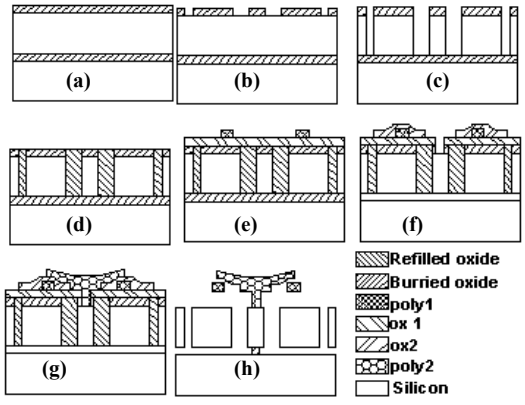

***Figure 1**: SOI plus hinges fabrication process. (a) Oxidize wafer to create mask layer. (b) Pattern oxide. (c) Etch Si. (d) Refill Cavities with oxide. (e) Deposit oxide 1, poly1 and pattern poly1. (f) Deposit and pattern oxide 2. (g) Deposit and pattern poly 2. (h) HF etch of oxide*

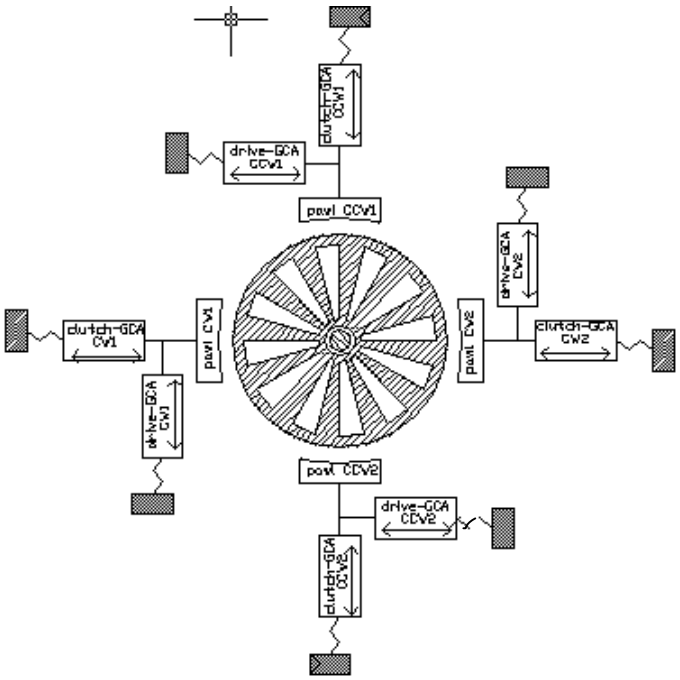

Figure 2: Diagram of Rotary Inchworm Motor

axle, and the GCA's have been patterned onto the front side of the silicon wafer using a photoresist, the wafer is refilled with silicon dioxide. First oxide layer is deposited after which a polysilicon layer is deposited and patterned. A second oxide layer is deposited and contacts to the rotor axle are opened. Another layer of polysilicon is deposited and patterned to restrain the rotor from leaving the axle. Finally, a timed HF etch is performed to release the structures followed by a critical-point dry.

II.2 Rotary Motor Description

The rotary inchworm motor consists of a free moving rotor that is pin-joined to the wafer via an axle and four closing gap actuators (GCA). Two of the diametrically opposite GCA's (CW1 And CW2) as shown in figure2, are used to thrust the rotor in the clockwise direction, while the other two GCA's (CCW1 and CCW2) are capable of driving the rotor in the counterclockwise direction and are energized separately.

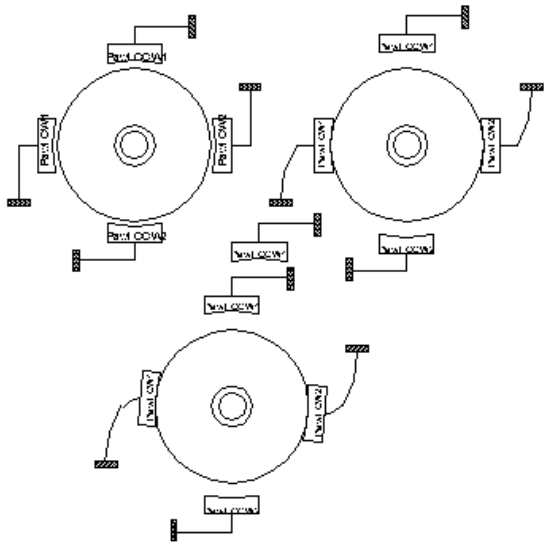

Figure 3: Diagram of Rotary Inchworm motor cycle for the clockwise rotation. (a) Pawl sCW1 and CW2 at initial position. (b) Pawls CW1 and CW2 engage to the motor. (c) Pawls CW1 and CW2 pull the free rotor in the clockwise direction

Due to fabrication constraints, a minimum of 2μm of clearance between the rotor and its axle is imposed. To avoid the backlash upon engaging one GCA's pawl onto the rotor and to overcome the consequent rubbing of the rotor with the axle, two such pawls are used to drive the rotor. In addition, the two diametrically opposite pawls offer a symmetrical output torque from the rotor. As shown in figure 3, to drive the rotor in the clockwise direction, GCA's CW1 and CW2 are energized and thus the pawls attach to the rotor after which they pull the rotor in the clockwise direction. The GCA's are then de-energized and go back to their initial position. Now that the rotor has deflected through an angle θ, the cycle goes on.

II.3 Actuator Design and Analysis:

As shown in figure 4, the gap closing actuator consists of N parallel capacitors of length l, separation distance g1, and thickness t. The right plates of the capacitors are connected together to form a fork that engages with the rotor via the clutch, while the left plates of the capacitors are linked together and anchored onto the substrate. When a voltage is applied to the capacitors, the right plates are attracted to the fixed left plates; thus moving the fork to the right and consequently turning the rotor in the clockwise direction. A small anchored plate, energized with the same potential as the right capacitor plates, is implemented to limit the motion of the fork so that the capacitors will not blow out upon contact of their right and left plates. A spring beam structure is attached to the right plates to insure their return to their initial position when the voltage drops to zero.

The forces acting on the rotor are the actuation forces generated from the GCA's in addition to the friction forces on the rotor. Thus $F_{net}=F_{g1}+F_{g2}+F_{spring}+F_{damp}+F_{fric}$

where F_{net} is the net force acting on the circumference of the rotor, F_{g1} and F_{g2} are the electrostatic forces acting on the right and left side of the right plate, F_{spring} is the restoring spring force, F_{damp} is the damping force, and F_{fric} is the frictional force on the rotor. The above forces are calculated as follows:

$$F_{g1} = \frac{1}{2}\varepsilon N V^2 \frac{tl}{(g_1 - x)^2} \dots (1)$$

$$F_{g2} = -\frac{1}{2}\varepsilon N V^2 \frac{tl}{(g_2 - x)^2} \dots (2)$$

where ε is the permissivity constant of air, N is the number of capacitors, V is the applied voltage, t is the thickness of the capacitor, l is the length of the capacitor, g_1 is the separation between the plates of a capacitor, g_2 is the separation between the plates of two consecutive capacitors, and x is the distance each right plate has moved. Also,

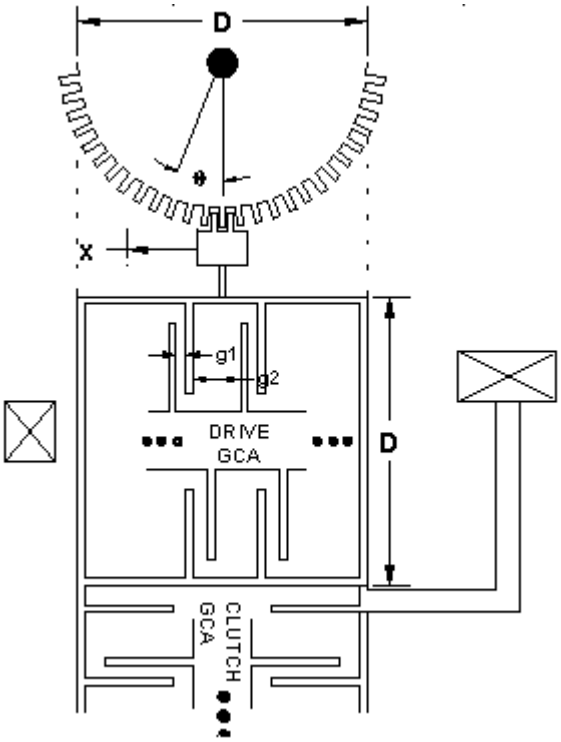

Figure 4: Sketch of the Rotary Inchworm Motor rotor and GCA drive and clutch actuators

$$F_{spring} = K_{spring}\, x \ldots (3)$$

$$F_{damp} = \frac{-b\dot{x}}{(g1-x)^3} \ldots (4)$$

$$Ffric = -\mu\frac{mg}{2} \quad (considering \quad half \quad the \quad rotor) \ldots (5)$$

where K_{spring} is the spring constant, b is the damping constant, μ is the coulomb friction coefficient, m is the mass of the rotor, and g is the gravitational acceleration.

The minimum voltage required to close the gap between the upper and lower plates of the capacitor is given by [2]:

$$Vpi = \sqrt{\frac{8k_{spring}g_1^3}{27\varepsilon t^3 lN}} \ldots (6)$$

For a lateral movement of x, the rotor is displaced Dθ/2, where D is the diameter of the plate and θ is the angular rotation of the rotor. Now, writing Newton's second law for the rotor:

$$J\ddot{\theta} = M_{ext} \ldots (7)$$

$$or \quad J\ddot{\theta} = D\left\{\left(\frac{1}{2}\varepsilon NV^2 tl\right)\left[\frac{1}{(g_1-\frac{D\theta}{2})^2} - \frac{1}{(g_2-\frac{D\theta}{2})^2}\right] - K_{spring}\frac{D\theta}{2} - \frac{b\frac{D}{2}\dot{\theta}}{(g1-\frac{D\theta}{2})^3} - \mu\frac{mg}{2}\right\} \ldots (8)$$

II.4 Torque output and Torque Density of the Rotor:

Since the electrostatic forces of the Drive GCA are inversely proportional to the square of the gap between the capacitor plates (see equations 1 & 2), the forces increase as the capacitors are energized (assuming the spring restoring forces do not offset the electrostatic forces). Thus, in order to get an estimate of the torque output of the rotor, the initial gap separation represents a lower limit of this torque.

In order to optimize the use of area surrounding the rotor, an area of D^2 μm^2 is allocated for each drive GCA and an equal area is allocated for each clutch GCA. The width of the plates forming the GCAs is assumed to be 3μm, which is the minimum resolution of the SOI process. To maximize the electrostatic forces, a smaller gap is required. As a matter of fact, the gap g1 is designed to be 4μm. According to Pister et al. [2], the gap g2 should be at least 2.8 times g1 to overcome the parasitic effects of F_{g2}. Consequently; g2 is designed to be 12μm. Taking into account that the left plates of the capacitors are to be anchored to the substrate, the process design rules imply that they should occupy a minimum width of 80 μm. A room of (D-80)μm is left for the length of the capacitors and to avoid pull in due to moment, the capacitors are built in two symmetrical columns. The total number of capacitors within a drive GCA becomes D/11, where D is in μm. The starting output torque and the torque density could be expressed as follows:

$$\therefore (F_e)_{x=0} = F_{g1} + F_{g2} = \frac{1}{2}\varepsilon V^2 tLN\left(\frac{1}{(g_1-x)^2} - \frac{1}{(g_2-x)^2}\right) \ldots (9)$$

$$or \quad (F_e)_{x=0} = \frac{1}{2}\varepsilon V^2 t\left(\frac{D-80}{2}\right)\frac{D}{11}\left(\frac{1}{(g_1)^2} - \frac{1}{(g_2)^2}\right) \ldots (10)$$

$$but \quad F_{fric} = \mu\frac{mg}{2} = \frac{1}{2}\mu\frac{\pi D^2}{4}t\rho g \ldots (11)$$

$$\Rightarrow T_{initial} = D\left\{\frac{1}{2}\varepsilon V^2 t\frac{(D-80)}{2}\frac{D}{11}\left(\frac{1}{(g_1)^2} - \frac{1}{(g_2)^2}\right) - \frac{1}{2}\mu\frac{\pi D^2}{4}t\rho g\right\} \ldots (12)$$

$$\therefore \tau = \frac{T_{initial}}{Area} = \frac{T_{initial}}{(5D)^2} \ldots (13)$$

$$or \quad \tau = \frac{1}{25D}\left\{\frac{1}{2}\varepsilon V^2 t\frac{(D-80)}{2}\frac{D}{11}\left(\frac{1}{(g_1)^2} - \frac{1}{(g_2)^2}\right) - \frac{1}{2}\mu\frac{\pi D^2}{4}t\rho g\right\} \ldots (14)$$

where F_e is the net electrostatic forces, ρ is the density of silicon and τ is the torque density.

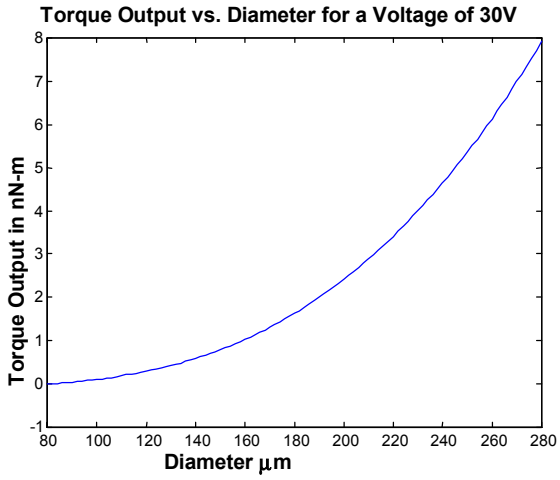

Figure 5: Torque output of the motor in nN-m vs. rotor diameter in μm

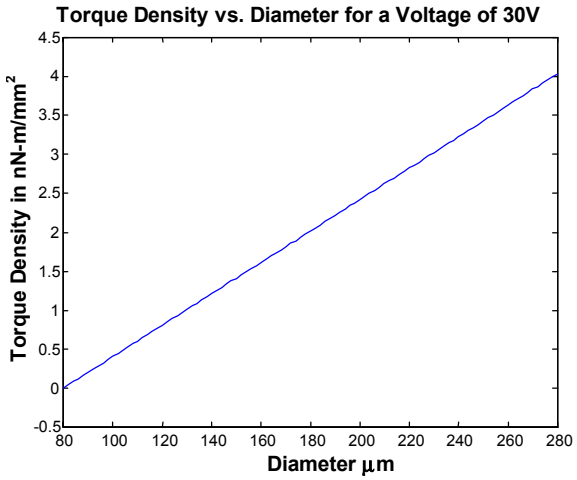

Figure 6: Torque density of the motor in nNm/mm^2 vs. diameter in µm

III. Test Structures and Expected Results

Linear inchworm motors, which constitute the subcomponents of the current design, have been successively designed and fabricated by Pister et al [2]. Using Silicon-on-oxide plus hinges process, several rotary inchworm motors of various diameters are going to be built and tested under varying voltages and frequencies. Since such a process has an aspect ratio of 25:1, structures of 50µm thickness are expected. As shown in figure 5, it is expected that as the diameter increases, the output torque of the rotor increase consequently. The torque density is also expected to increase with the rotor diameter (see figure 6). For instance, for one test structure with rotor diameter of 200µm, the dimensions of the motor are 1mmx1mmx60µm, the expected output torque is 2.4nN-m, and the torque density is 2.4nN-m/mm^2. For another test structure with rotor diameter of 150µm, the dimensions of the motor are 750µmx750µmx60µm, the theoretical minimum torque output is 0.8nN-m, and the torque density is 1.42nN-m/mm^2. At low frequencies, the motor is expected to behave like a stepper motor whose step θ_s is the lateral displacement of the drive GCA divided by the rotor radius (D/2) with the speed increasing linearly as frequency increases.

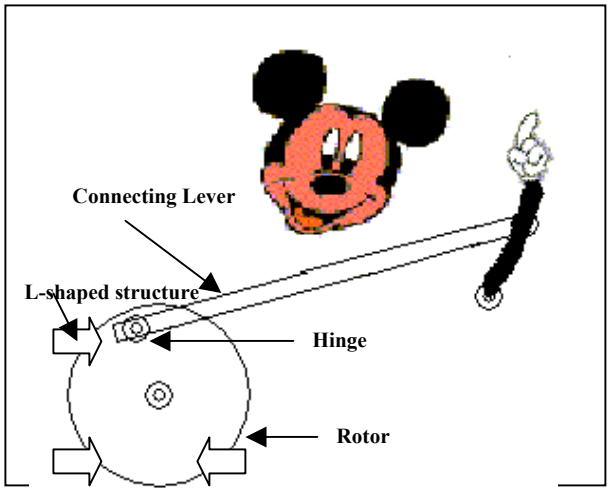

Figure 7: Mickey Mouse waving his hand!

One "cool" application of this Rotary Inchworm motor is to wave Mickey Mouse's hand. As shown in Figure 7, the Rotary Inchworm Motor is used to drive a four bar mechanism that causes the arm of the Mickey Mouse to oscillate back and forth. The arm and the rotor are etched and pinned on the SOI wafer while the connecting lever is built from poly 1 layer. The connecting lever is hinged respectively to the arm and the rotor using pins fabricated using poly 2 through holes etched into the poly 1 lever and onto the SOI wafer. The arm is locked onto its axle by a T-shaped poly2 structure via a contact to its axle made of poly 2 while the rotor is restrained from falling off its axle by three L-shaped poly2 structures attached to the SOI wafer. This avoids the interference between the rotor and the and the lever which would be the case had a T-shaped structure been used instead

IV. Conclusion

A novel Rotary Inchworm motor has been successfully designed using a standard Silicon-on-Insulator (SOI) plus hinges process. This motor is thought to be an important achievement in the field of electrostatic micro-motors when fabricated. Its torque output is decoupled from the rotational speed, thus it could achieve high torques and high speeds at the same time. In addition, it has higher torque and torque density than previous designs. No serious problems that might cause the motor not to work are currently foreseen.

Upon fabrication and testing of the first generation of the new inborn of rotary inchworm micro-motors, extensive research would be undertaken to optimize the design. Moreover, upon verifying that such a design is powerful as suggested, new research ideas in the field of *Micro Robotics* would be inspired. An application of this motor to wave Mickey Mouse's hand has been suggested. Nevertheless, micro-cars or even micro-flying vehicles might become reality!

References

[1] E. J. Gracia and J. J. Sniegowski, "Surface micromachined microengines," Sensors and Actuators A, vol. 48, 1995 pp.203-214

[2] Richard Yeh, Seth Hollar, and Kristofer S. J. Pister, "Single mask, large force, and large displacement electrostatic linear inchworm motors," IEEE 2001, pp. 260-264

[3] L. S. Fan, Y. C. Tai, and R.S. Muller, "IC-processed electrostatic micromotors," Sensors and Actuators, vol. 20, pp.41-47, 1989

[4] J. J. Sniegowski and E. J. Gracia, "Surface-micromachined gear train drive by an on-chip electrostatic microengine," IEEE Electron Device Letters, vol. 17, no. 7, July 1996

[5] E. J. Gracia and J. J. Sniegowski, "Surface micromachined microengine as the driver for mechanical gears," in Proc. 8th Int. Conf. Solid-State Sensors and Actuators Eurosensors IX (Transducers '95), Stockholm, Sweden, June 25-29, 1995, vol. 1, pp. 365-368

[6] Gregor T.A. Kovacs, "Micromachined Transducers Sourcebook," McGraw Hill 1998, pp. 284-288

[7] L. G. Frechette, S. F. Nagle, R. Ghodssi, S. D. Umans, M. A. Schmidt, and J. H. Lang, "An electrostatic induction micromotor supported on gas-lubricated bearings," IEEE 2001, pp. 284-288

[8] Marc Madou, "Fundamentals of Microfabrication," CRC 1997,pp.416-420